AGE (2012) 34:95–109
DOI 10.1007/s11357-011-9223-7

MnSOD activity regulates hydroxytyrosol-induced extension of chronological lifespan

Ehab H. Sarsour · Maneesh G. Kumar · Amanda L. Kalen · Monali Goswami · Garry R. Buettner · Prabhat C. Goswami

Received: 27 October 2010 / Accepted: 15 February 2011 / Published online: 8 March 2011

Abstract Chronological lifespan (CLS) is defined as the duration of quiescence in which normal cells retain the capacity to reenter the proliferative cycle. This study investigates whether hydroxytyrosol (HT), a naturally occurring polyphenol found in olives, extends CLS in normal human fibroblasts (NHFs). Quiescent NHFs cultured for a long duration (30–60 days) lose their capacity to repopulate. Approximately 60% of these cells exit the cell cycle permanently; a significant increase in the doubling time of the cell population was observed. CLS was extended in quiescent NHFs that were cultured in the presence of HT for 30–60 days. HT-induced extension of CLS was associated with an approximately 3-fold increase in manganese superoxide dismutase (MnSOD) activity while there was no change in copper–zinc superoxide dismutase, catalase, or glutathione peroxidase protein levels. Quiescent NHFs overexpressing a dominant-negative mutant form of MnSOD failed to extend CLS. HT suppressed age-associated increase in mitochondrial ROS levels. Results from spectroscopy assays indicate that HT in the presence of peroxidases can undergo catechol–semiquinone–quinone redox cycling generating superoxide, which in a cellular context can activate the antioxidant system, e.g., MnSOD expression. These results demonstrate that HT extends CLS by increasing MnSOD activity and decreasing age-associated mitochondrial reactive oxygen species accumulation.

Keywords Chronological lifespan · Ageing · Manganese superoxide dismutase · Quiescence · Hydroxytyrosol · Mitochondria

Abbreviations

AdmMnSOD	Adenoviruses carrying a dominant-negative form of human MnSOD cDNA
CLS	Chronological lifespan
CuZnSOD	Copper–zinc superoxide dismutase
EcSOD	Extracellular superoxide dismutase
EPR	Electron paramagnetic resonance
GPx	Glutathione peroxidase
HT	Hydroxytyrosol
MnSOD	Manganese superoxide dismutase
MOI	Multiplicity of infection
NHFs	Normal human fibroblasts
PI	Propidium iodide
ROS	Reactive oxygen species

Electronic supplementary material The online version of this article (doi:10.1007/s11357-011-9223-7) contains supplementary material, which is available to authorized users.

E. H. Sarsour · M. G. Kumar · A. L. Kalen · M. Goswami · G. R. Buettner · P. C. Goswami (✉)
Free Radical and Radiation Biology Division, Department of Radiation Oncology, The University of Iowa, Iowa City, IA 52242-1181, USA
e-mail: prabhat-goswami@uiowa.edu

Introduction

Preservation of the regenerative capacity of normal cells is imperative for tissue renewal and repair of damage. It is well-known that human somatic cells have a finite lifespan before undergoing irreversible growth arrest. The most widely studied theory of cellular lifespan is replicative senescence, also known as the "Hayflick limit" (Hayflick and Moorhead 1961) or "telomere shortening theory of ageing" (Henderson and Larson 1991). Replicative senescence is measured as the finite number of cell divisions ("mitotic counting") prior to exhibiting irreversible growth arrest. Several studies have shown "telomere attrition" as one of the main mechanisms of replicative senescence, while maintenance of telomere length prevents or delays replicative senescence (Bodnar et al. 1998; Vaziri and Benchimol 1998; Wright et al. 1996).

Quiescent (G_0) human somatic cells are also known to exhibit age-dependent loss in their regenerative capacity. This phenomenon was also observed in yeast. *Saccharomyces cerevisiae* cultured in stationary phase (G_0, quiescent) for a long duration were unable to divide (Harris et al. 2003). The authors referred to this mode of cellular ageing as chronological lifespan (CLS). We and others have shown that quiescent human fibroblasts cultured for a long duration were unable to proliferate following replating at a lower cell density (Allsopp et al. 1995; Munro et al. 2001; Sarsour et al. 2005; Sitte et al. 1998). We observed that quiescent fibroblasts lost their proliferative capacity (measured as percentage of S phase at 48 h following replating of cells at a lower cell density) beginning from 30 days of quiescence; a maximal drop in S phase percentage was observed in cells replated from 60 days of quiescence (Sarsour et al. 2005). The decrease in S phase was not due to cell death or changes in telomerase activity. Mid-lifespan fibroblasts kept in quiescence for 7–12 weeks lost their proliferative capacity, yet there were no detectable shortening of telomere (Allsopp et al. 1995; Munro et al. 2001; Sitte et al. 1998). Results from these previous studies suggest the presence of telomere-independent pathways that influence cellular lifespan.

An earlier study in *S. cerevisiae* demonstrated that overexpression of manganese superoxide dismutase (MnSOD) extends CLS, while the same treatment reduced replicative lifespan (Fabrizio et al. 2004; Harris et al. 2003). MnSOD is a redox enzyme that is nuclear encoded; it is localized to the mitochondrial matrix where it removes mitochondrial generated superoxide thereby influencing the redox environment of the cell (Buettner et al. 2006). The redox sensitivity of longevity is also demonstrated in *Drosophila* and *Caenorhabditis elegans* (Orr et al. 2003; Sohal et al. 1995; Sun et al. 2002; Taub et al. 1999). Transgenic mice overexpressing mitochondrial-targeted catalase showed an extension of the median and maximal lifespan by approximately 20% (Schriner et al. 2005). Consistent with these reports, we have shown previously that MnSOD overexpression extends CLS in human normal skin fibroblasts (Sarsour et al. 2005). MnSOD-induced extension of CLS was accompanied with a suppression of age-associated abnormalities in mitochondrial morphology and ROS levels (Sarsour et al. 2010).

Small molecular weight chemicals of botanical origin have been used as antioxidants to quench ROS. Hydroxytyrosol (2-(3,4-dihydroxyphenyl) ethanol) is a hydrophilic polyphenol commonly found in olives; olive oil is a common ingredient of the Mediterranean diet (Rodriguez et al. 2009). The use of olive oil in the diet is believed to be associated with a lower incidence of cancer and cardiovascular diseases in the Mediterranean population (Fabiani et al. 2008; Visioli et al. 1998). Potential benefits of hydroxytyrosol (HT) are also suggested for preventing diabetes, vascular damage, and influenza (Jemai et al. 2009; Jemai et al. 2008; Yamada et al. 2009). A recent study showed activation of longevity proteins (SIRT and FoxO) in heart cells of HT-fed rats, suggesting that HT could impact ageing (Mukherjee et al. 2009). The mechanisms regulating the beneficial effects of HT are not completely understood. Earlier studies have shown that HT in the presence of peroxidase/H_2O_2 (PBS, pH 7.4) undergoes oxidation initiating catechol–quinone coupling to yield methanooxocinobenzodioxinone (De Lucia et al. 2006; Vogna et al. 2003). Although this oxidative chemistry of HT supports the proposed role of catechols (olive phenols) as scavengers for H_2O_2, it is unclear if such a chemical reaction occurs in biological system at a rate that is significant.

The present work demonstrates that HT increases MnSOD activity, inhibits an age-associated increase

in mitochondrial ROS levels, and extends CLS of normal human skin fibroblasts. The antioxidant properties of HT could be due to its ability to undergo catechol–semiquinone–quinone redox cycling generating superoxide, which in a cellular context activates the expression of MnSOD.

Materials and methods

Cell culture

Human normal skin fibroblasts (AG01522D) from a 3-day-old male of non-fetal origin were obtained from Coriell Cell Repositories. Cells were cultured in Dulbecco's modified Eagle's medium containing 10% fetal bovine serum and antibiotics in incubators with a controlled temperature of 37°C, 5% CO_2, 95% humidity, and atmospheric oxygen. All experiments with normal human skin fibroblasts (NHFs) were performed using passages 7–8, except long-term experiments (>50 days) were done using passages 3–4.

Chronological lifespan assay

One million cells per T-75 tissue culture flask were cultured in regular medium. Cells with less than 5% S phase were considered a quiescent culture. Quiescent cultures were fed every 3 days with regular and HT-containing medium. Measurements of proliferative potential were performed by first trypsinizing the quiescent cell cultures and replating cells at a lower density, and then counting cell numbers at different days. Cell numbers were counted using a Coulter Counter (Beckman-Coulter). To calculate population-doubling time, we applied trend/regression plots of exponential growth and then used the equation $T_d = 0.693t/\ln(N_t/N_0)$ where t represents time in days, N_t represents cell numbers at time t, and N_0 represents initial number of cells.

The method used to measure CLS in our study is slightly different than the approach used to measure CLS in yeast. Mammalian cells are well-known to arrest growth upon contact inhibition, while in yeast aging research of CLS starvation is commonly used to induce quiescence. Literature reports suggest that in mammalian cells, starvation may induce cell death (e.g., autophagy). Therefore, we used contact inhibition to induce quiescence and fed cells every 3 days while in culture.

Flow cytometry assays

Ethanol-fixed cells were treated with RNase A for 30 min followed by staining with propidium iodide. Flow cytometry analysis of DNA content and percent cell cycle phase distributions were performed following our previously published methods (Menon et al. 2003; Sarsour et al. 2005).

For the bromodeoxyuridine (BrdU)-labeling assay, control and HT-treated NHFs were incubated with 10 μM of BrdU for 30 min and cells were collected by trypsinizing the monolayer cultures. Cell pellets were washed in PBS and fixed in 70% ethanol for 24 h at 4°C. Isolated nuclei were incubated with anti-BrdU primary antibody (1:50, BD Biosciences) followed by incubation with FITC-conjugated goat anti-mouse IgG (1:50, BD Biosciences). Nuclei were then treated with RNase A (0.1 mg/mL) for 30 min and counterstained with 35 μg/mL propidium iodide for 1 h. Propidium iodide and FITC fluorescence were analyzed on a FACScan flow cytometer (BD Biosciences); red fluorescence from propidium iodide was detected using 488-nm excitation and 640-nm long-pass filter (FL2), and green fluorescence from FITC was detected through a 525-nm band pass filter (FL1). Data from a minimum of 20,000 nuclei were acquired in list mode and were processed using FlowJo software (Tree Star, Inc.). Dual-parameter propidium iodide vs. log-FITC histograms were used to identify three compartments: BrdU-positive nuclei representing S phase; BrdU-negative nuclei representing G_1 and G_2 phases. The number of nuclei in each compartment was calculated and expressed as percentage of total gated population.

Flow cytometry measurements of MitoSOX and MitoTracker fluorescence (Invitrogen) were performed to determine mitochondrial ROS levels in control and HT-treated NHFs (Sarsour et al. 2010; Sarsour et al. 2008). Monolayer cultures were incubated with Hanks buffered salt solution containing 10 μM MitoSOX and 0.5 μM MitoTracker green. Cells were collected by trypsinizing the monolayer cultures and filtered through nylon-mesh. Flow cytometry measurements were performed using 488-nm excitation laser and 585/42-

nm emission filter for MitoSOX, and 530/30-nm emission filter for MitoTracker green fluorescence. Mean fluorescence intensity (MFI) was calculated using FlowJo software. The MFI of MitoSOX was normalized relative to the MFI of MitoTracker green and percent change calculated relative to untreated control; autofluorescence was used for background correction.

SOD activity assay

Total cellular protein extracts were assayed for MnSOD and CuZnSOD activities following a previously published gel-electrophoresis assay (Beauchamp and Fridovich 1971; Sarsour et al. 2010; Sarsour et al. 2008). Briefly, control and HT-treated NHFs were harvested by scraping the monolayers and cell pellets were resuspended in phosphate buffer (pH 7.8). Total cellular protein extracts were prepared by sonicating cell suspensions on ice (Vibra Cell Sonicator with cup attachment, Sonics and Materials Inc.). Equal amounts of protein were separated by native gel-electrophoresis, and SOD activity assayed by incubating the gel with nitroblue tetrazolium. Sodium cyanide (0.75 mM) was used to distinguish CuZnSOD activity from MnSOD activity. A computerized digital imaging system (Epson dual-light digital scanner, Epson America) and ImageJ software were used to calculate fold change in SOD activity.

Immunoblotting assay

Equal amounts of protein were separated by 12.5% SDS-PAGE and electrotransferred by semidry blotting onto a nitrocellulose membrane. Blots were incubated with rabbit anti-human polyclonal antibodies against MnSOD (1:1,000, Upstate), CuZnSOD (1:1,000 Millipore), catalase (1:1,000, Athens Research and Tech.), and glutathione peroxidase 1 (1:1,000, Millipore). Immunoreactive bands were detected by an enhanced chemiluminescence kit (GE Healthcare) and X-ray film. Epson dual-light digital scanner (Epson America Inc.) and ImageJ software were used to quantify results. The integrated density value was obtained by integrating the entire pixel values in the area of one band after correction for background. Actin protein levels were used for loading corrections, and fold change was calculated relative to untreated control.

Adenoviral infection

Replication-deficient adenoviruses containing cytomegalovirus promoter driven dominant-negative mutant form of human MnSOD cDNA (Zhang et al. 2006) were used to infect quiescent NHFs following our previously published method (Sarsour et al. 2008). Site-directed mutagenesis was used to generate the mutant form of human MnSOD that has a histidine to leucine substitution at amino acid 26 (Zhang et al. 2006). After incubation for 24 h with the virus, the media was changed to full media containing 10% serum. MnSOD protein levels and activities were measured to determine transgene expression.

Quantitative RT-PCR assay

Real-time PCR assay was applied to measure MnSOD mRNA levels in control and HT-treated NHFs following our previously published protocol (Sarsour et al. 2010). One microgram of RNA was reverse transcribed using the high-capacity cDNA Archive Kit (Applied Biosystems). Real-time PCR assay was performed using primers specific to MnSOD open reading frame, and 18S ribosomal RNA: MnSOD forward primer, 5′-GGCCTACGTGAACAACCTGAA-3′, reverse primer, 5′-CTGTAACATCTCCCTTGGCCA-3′; amplicon size 70 bp. PCR cycle parameters (SetpOne Plus, Applied Biosystems) were set at 95°C for 10 min, and 40 cycles of 95°C for 15 s and 60°C for 1 min. Linear range threshold of amplification was selected to calculate the cycle threshold (CT). The relative mRNA levels were calculated as follows: ΔCT (sample)=CT (mRNA of sample)—CT (18S); ΔΔCT=ΔCT (post-treatment time point)—ΔCT (control); relative expression=$2^{-\Delta\Delta CT}$.

Electron paramagnetic resonance spectroscopy

Electron paramagnetic resonance (EPR) spectroscopy was done at room temperature using a Bruker EMX EPR spectrometer equipped with a TM cavity and a quartz flat cell. Samples (500 μL total volume) were prepared using 1 mM HT in PBS (pH 7.4) and 100-μM hydrogen peroxide with either 20-mU horseradish peroxidase, 20 mU lactoperoxidase, 5-μM hemoglobin, or 5-μM myoglobin. EPR-parameters for the semiquinone spectra were: 20 mW power, 2.52×10^5 receiver gain, modulation amplitude of 2 G, scan rate

of 15 G/41.9 s, time constant of 0.819 s, and an average of 25 scans. Simulated EPR spectra were generated using WINSIM 1.0 EPR software.

UV spectroscopy

UV spectra were recorded with a Hewlett–Packard 8,453 diode array spectrometer. HT (250 μM) was incubated in near-neutral buffer in absence or presence of superoxide dismutase (0.38 mg/mL; 5,060 Units/mg bovine SOD, Sigma) and the change in absorbance was measured at 300 nm (the spectral region for the quinone form of HT) for 20 min.

Statistical analysis

Statistical analysis was done using the one and two-way analysis of variance with Tukey's honestly significant difference test; student *t* test was used for experiments with less than three groups. Homogeneity of variance was assumed with 95% confidence interval level. Results from at least $n \geq 3$ with $p < 0.05$ were considered significant. All statistical analyses were done using SPSS version 17 and/or SigmaPlot version 11.

Results

Hydroxytyrosol extends chronological lifespan of normal human fibroblasts

CLS is defined as the duration of quiescence in which normal cells retain the capacity to divide following reentry into the proliferative cycle. The capacity of quiescent cells to divide diminishes with age. In this study, we measured changes in the percentage of S and G_2 phases in cells replated from different days of quiescence as well as population-doubling times to assess CLS. To determine if HT extends CLS, quiescent NHFs were cultured in medium containing 1–200 μM HT for 15–30 days, and replated at a lower cell density. The percentage of cell cycle phases was determined by flow cytometry measurements of DNA content at 24-h post-replating. Cells replated from 15-day quiescence showed approximately 40% S and G_2 phases in control and HT-treated (1–200 μM) cells (Fig. 1b). Control cells replated from 30-day quiescence showed a significant decrease in the percentage of S and G_2 phases compared with cells replated from 15-day quiescence (10% vs. 40%). Interestingly, cells replated from 30-day HT-treated quiescent NHFs showed a consistently higher percentage of S and G_2 phases compared with the 30-day untreated control cells. These results showed that the percentage of S and G_2 phases decreased in cells replated from 30- vs. 15-day quiescent NHFs, while cells replated from HT-treated quiescent NHFs consistently maintained a higher percentage of S and G_2 phases (Fig. 1b). HT-induced extension of CLS was also evident in cells replated from 30-day quiescent cells that were incubated with 300 μM of HT (Fig. 1 in the Electronic supplementary material).

HT-induced extension of CLS was further evident from the results presented in Fig. 1c. Control and HT-treated 15- and 30-day quiescent NHFs were replated and cell numbers determined at 2-, 4-, and 6-day post-plating. We used the linear plot to determine if age-associated changes in the proliferative capacity of quiescent cells could also be due to a change in the lag phase of the growth curve. It appears that upon reentry to the proliferative cycle, 30-day-old quiescent cells have a longer lag period compared with cells replated from 15-day-old quiescent cells (Fig. 1c (compare right vs. left panels)). Thirty-day HT treatments did not appear to change this lag period. We applied trend/regression plots of exponential growth and then used the equation ($T_d = 0.693\ t/\ln(N_t/N_0)$) to calculate doubling time. Cells replated from 15-day quiescent cultures exhibited population-doubling time of 42 h, while cells replated from 30-day quiescent cultures showed population-doubling time of 51 h (Fig. 1c). NHFs replated from 30-day HT-treated cells showed population-doubling time of 38 h, which was comparable to a population-doubling time of 42 h in cells replated from 15-day control quiescent cultures. The doubling times calculated from the regression plots (Fig. 1c) were comparable to the doubling times calculated from the ln-linear plots (Fig. 2 in the Electronic supplementary material): 49.3 and 39.4 h for cells replated from 30-day control and HT-treated cells, respectively. HT-induced extension of CLS was also observed in 60-day quiescent cells (Fig. 2 in the Electronic supplementary material). These results indicate that HT maintained population-doubling time in 15-, 30-, and 60-day quiescent NHFs.

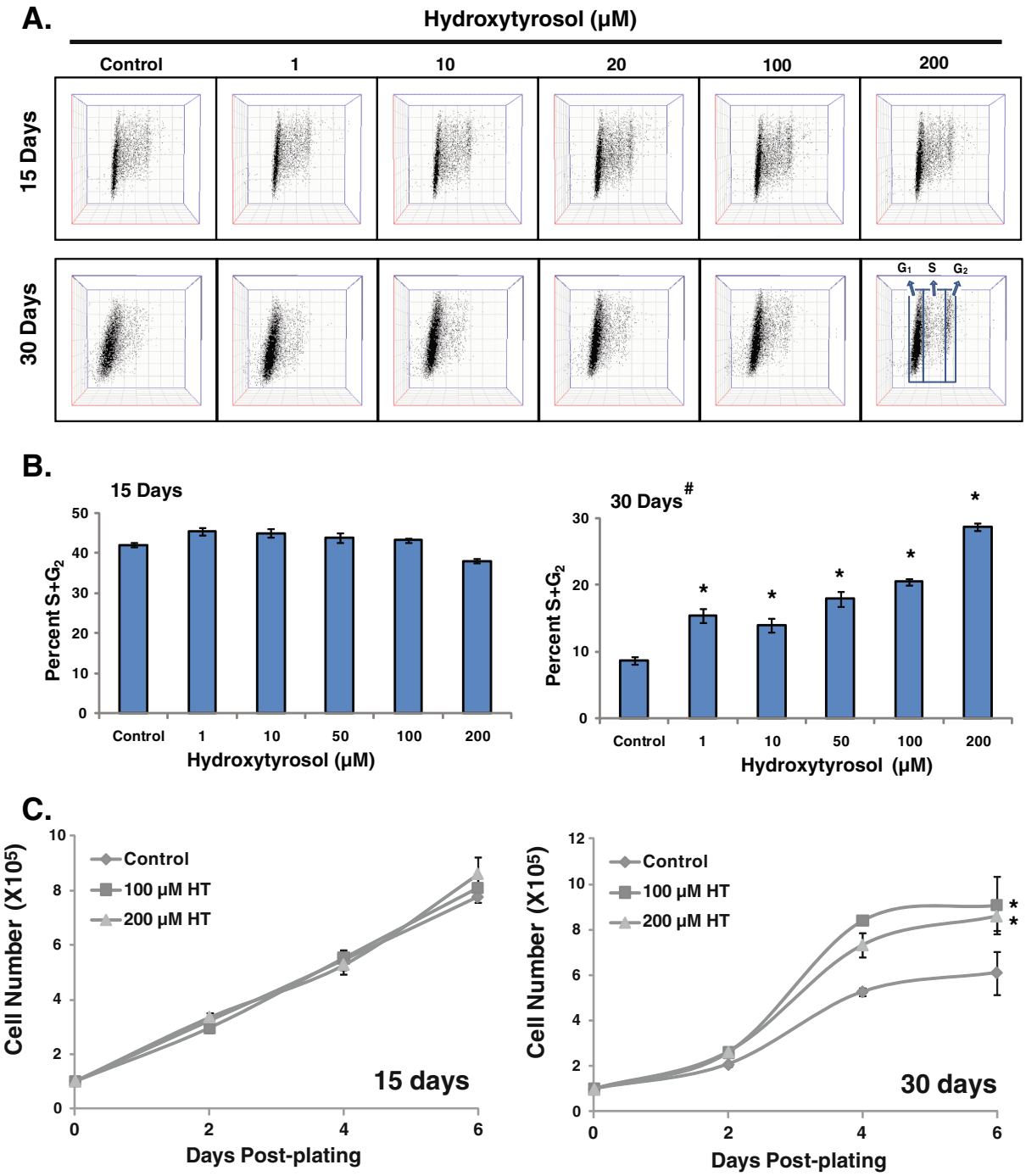

Fig. 1 Hydroxytyrosol extends chronological lifespan of normal human skin fibroblasts. Control and HT-treated 15- and 30-day quiescent cultures of NHFs were replated at a lower cell density and harvested at 24-h post-plating for flow cytometry analysis of DNA content: **a** representative dot plots of propidium iodide-stained cells exhibiting the DNA content of G_1, S, and G_2 phases; **b** the percentage of S and G_2 phases was calculated using FlowJo and ModFit software; **c** cell growth in cells replated from 15- and 30-day control and HT-treated NHFs. *Asterisks* indicate significant difference compared with untreated control; *number sign* indicates significant difference in cells replated from 30- vs. 15-day quiescent NHFs. $n=3$; $p<0.05$

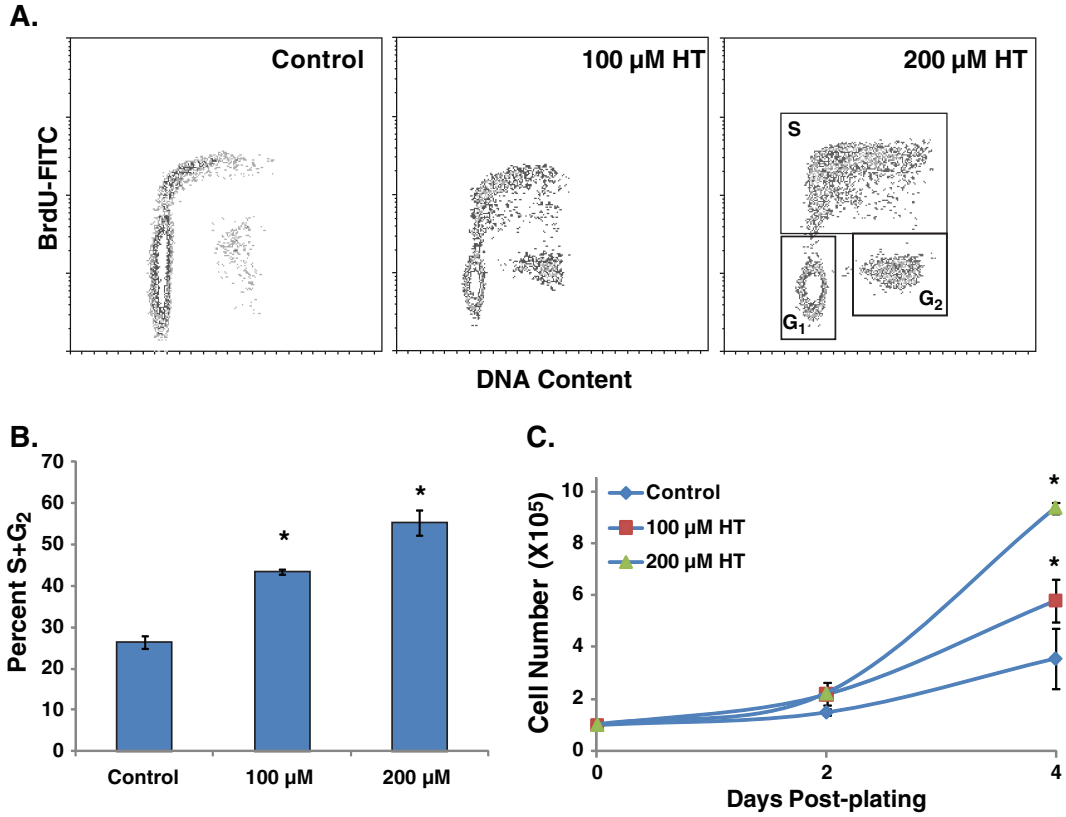

Fig. 2 Hydroxytyrosol extends chronological lifespan after long duration of quiescence. Sixty-day control and HT-treated quiescent cultures of NHFs were replated at a lower cell density and cell growth characteristics were measured by flow cytometry analysis of BrdU-labeled cells at 48-h post-plating: **a** representative BrdU vs. PI density plot of DNA content; **b** percentage of S and G_2 phases were evaluated using FlowJo and ModFit software; **c** cell numbers at 2- and 4-day post-plating. *Asterisks* indicate significant difference compared with untreated control. $n=3$; $p<0.05$

HT-induced extension of CLS was also apparent from results obtained from a dual-parameter flow cytometry assay. Quiescent NHFs were incubated with 100 and 200 μM of HT for 60 day and replated at a lower cell density. At 48-h post-plating, cells were incubated with BrdU for 30 min and analyzed for DNA content by flow cytometry measurements of propidium iodide and FITC fluorescence (Sarsour et al. 2005). Consistent with results shown in Fig. 1, control cells showed a significant decrease in the percentage of S and G_2 cells, approximately 20% compared with 70% S and G_2 phases in cells replated from 3-day quiescent NHFs. These cells exhibited a population doubling of 57 h (Fig. 2c). The percentage of S and G_2 in cells replated from HT-treated (100 and 200 μM) 60-day quiescent cultures were 40–50%, which is consistent with a lower population-doubling time of 38 and 32 h compared with 57 h in untreated control cells (Fig. 2b, c). These results demonstrate that HT extends CLS of NHFs.

MnSOD activity regulates hydroxytyrosol-induced extension of chronological lifespan

We have shown previously that overexpression of MnSOD in quiescent cultures protects NHFs from age-associated loss in proliferative capacity (Sarsour et al. 2005). To determine if HT-induced extension of CLS could be associated with changes in MnSOD activity, 15-day quiescent NHFs were treated with HT for 3 days and harvested for analysis of MnSOD expression. Results from western blot assays showed a dose dependent increase in MnSOD protein levels, which increased 3-fold in cells treated with 200 μM

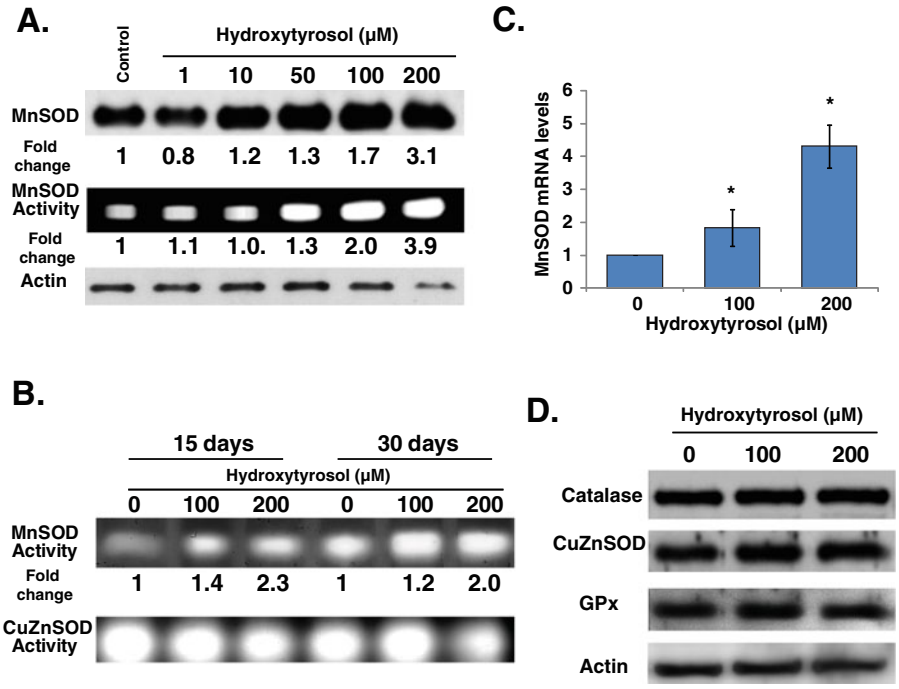

Fig. 3 Hydroxytyrosol increases MnSOD activity in quiescent NHFs. Immunoblotting and gel-electrophoresis assays for MnSOD protein levels and activity in quiescent NHFs that were incubated with HT for **a** 3, and **b** 15 and 30 days. Monolayer quiescent cultures of NHFs were fed with HT-containing fresh media every 3 days. Actin protein levels were used for loading correction; fold change was calculated first by adjusting for loading and then relative to untreated control. Sodium cyanide was used to distinguish between MnSOD and CuZnSOD activities. **c** Quantitative RT-PCR assay measuring MnSOD mRNA levels in 3-day control and HT-treated quiescent NHFs; fold change was calculated relative to 18S and untreated control. *Asterisks* indicate significant difference between control and HT-treated cells. $n=3$; $p<0.05$. **d** Immunoblot analysis of antioxidant enzymes at the end of 3-day HT-treated quiescent NHFs

HT (Fig. 3a). HT-induced increase in MnSOD protein levels correlated with a corresponding increase in its activity (Fig. 3a). The increase in MnSOD activity persisted in HT-treated 15- and 30-day quiescent cultures (Fig. 3b). It is interesting to note that while HT increased MnSOD activity, it did not increase CuZnSOD activity. HT-induced increase in MnSOD protein levels was associated with 2- to −4-fold increase in its mRNA levels (Fig. 3c). HT treatment of quiescent NHFs did not show any change in catalase, CuZnSOD, or GPx protein levels (Fig. 3d). HT induces MnSOD expression, while the same treatment did not affect protein levels of CuZnSOD, catalase, or GPx.

The role of MnSOD activity regulating CLS in HT-treated quiescent NHFs was further evident from the results presented in Fig. 4. Fifteen-day quiescent NHFs were infected with adenoviruses carrying a dominant-negative mutant form of human MnSOD cDNA (AdmMnSOD) (Zhang et al. 2006). Control, AdBgl-II-, and AdmMnSOD-infected quiescent NHFs were replated at a lower cell density and harvested at 24-h post-plating for flow cytometry analysis of DNA content (Fig. 4). MnSOD activity decreased more than 75% in quiescent NHFs over-expressing the dominant-negative mutant form of MnSOD compared with control and AdBgl-II-infected cells (Fig. 4 (inset)). The decrease in MnSOD activity in quiescent cultures was associated with a significant decrease in the percentage of S and G_2 cells following replating (approximately 15% S and G_2 compared with the 80% in control and AdBgl-II-infected cells; Fig. 4). AdmMnSOD-infected quiescent NHFs incubated with HT showed approximately 30% S and G_2 cells following replating (Fig. 4). MnSOD activity regulates CLS, and the HT-induced extension of CLS could be due to its ability to activate the expression of MnSOD.

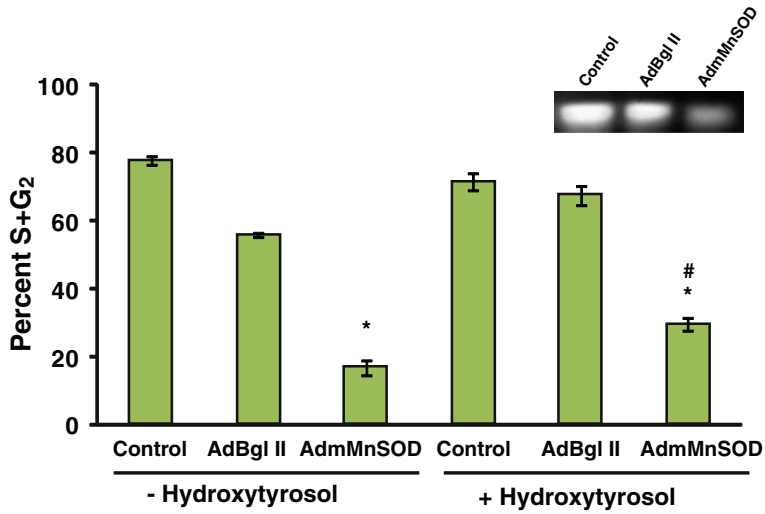

Fig. 4 MnSOD activity regulates hydroxytyrosol-induced extension of chronological lifespan. Quiescent NHFs were infected with 50 MOI of adenoviruses carrying a control vector (AdBgl II) or a dominant-negative mutant form of human MnSOD cDNA (AdmMnSOD). Forty-eight hours post-infection cells were incubated with 200 μM HT for 3 days. Uninfected control and infected cells were replated at a lower cell density and harvested at 24-h post-plating for flow cytometry analysis of DNA content. MnSOD activity was analyzed using native gel-electrophoresis assay. *Asterisks* indicate significant difference in AdmMnSOD-infected cells compared with control; *number sign* represents statistical significance between HT-treated AdmMnSOD-infected cells compared with AdmMnSOD-infected cells. $n=3$; $p<0.05$

Hydroxytyrosol suppressed age-associated increase in mitochondrial ROS levels

MnSOD is localized to the mitochondrial matrix where it removes mitochondrial generated superoxide. We have shown previously that age-associated increase in mitochondrial ROS levels negatively impact CLS (Sarsour et al. 2010). To determine if HT-induced increase in MnSOD activity alters mitochondrial ROS levels, 15- and 30-day control and HT-treated (100 and 200 μM) quiescent NHFs were incubated with MitoSOX and MitoTracker dyes. MitoSOX oxidation is sensitive to changes in mitochondrial ROS levels and MitoTracker fluorescence is commonly used to measure mitochondrial mass. There was no change in MitoTracker fluorescence in 30- vs. 15-day control and HT-treated quiescent NHFs, suggesting that there were no significant change in mitochondrial mass (or number) during 15- and 30-day of quiescence (Fig. 5a (right panel); Fig. 3 in the Electronic supplementary material). However, MitoSox fluorescence increased approximately 2-fold in 30- compared with 15-day quiescent cultures (Fig. 5a (left panel), b). Fifteen-day quiescent NHFs that were incubated with HT showed a significant decrease (25%) in MitoSox fluorescence compared with 15-day untreated control (Fig. 5c (left panel)). This property of HT was more pronounced in 30-day quiescent NHFs that exhibited approximately 50% decrease in MitoSox fluorescence compared with 30-day control (Fig. 5c (right panel)). These results showed that HT suppressed age-associated increase in mitochondrial ROS levels while the same treatments did not change mitochondrial mass.

Spectroscopy measurements of catechol–semiquinone–quinone redox cycling of hydroxytyrosol

HT in the presence of peroxidase undergoes oxidation to initiate catechol–quinone coupling (De Lucia et al. 2006; Vogna et al. 2003); hydroquinones and quinones are known to produce relatively stable semiquinone radicals (Bachur et al. 1978). EPR spectroscopy was used to examine semiquinone radical from the one-electron oxidation of HT. An EPR spectrum was observed when HT was incubated with horseradish peroxidase or lactoperoxidase, heme-containing enzymes that catalyze hydrogen peroxide-dependent one-electron oxidation, consistent with the formation of semiquinone radical from HT (Fig. 6a). This same semiquinone radical spectrum was also observed when HT was incubated with

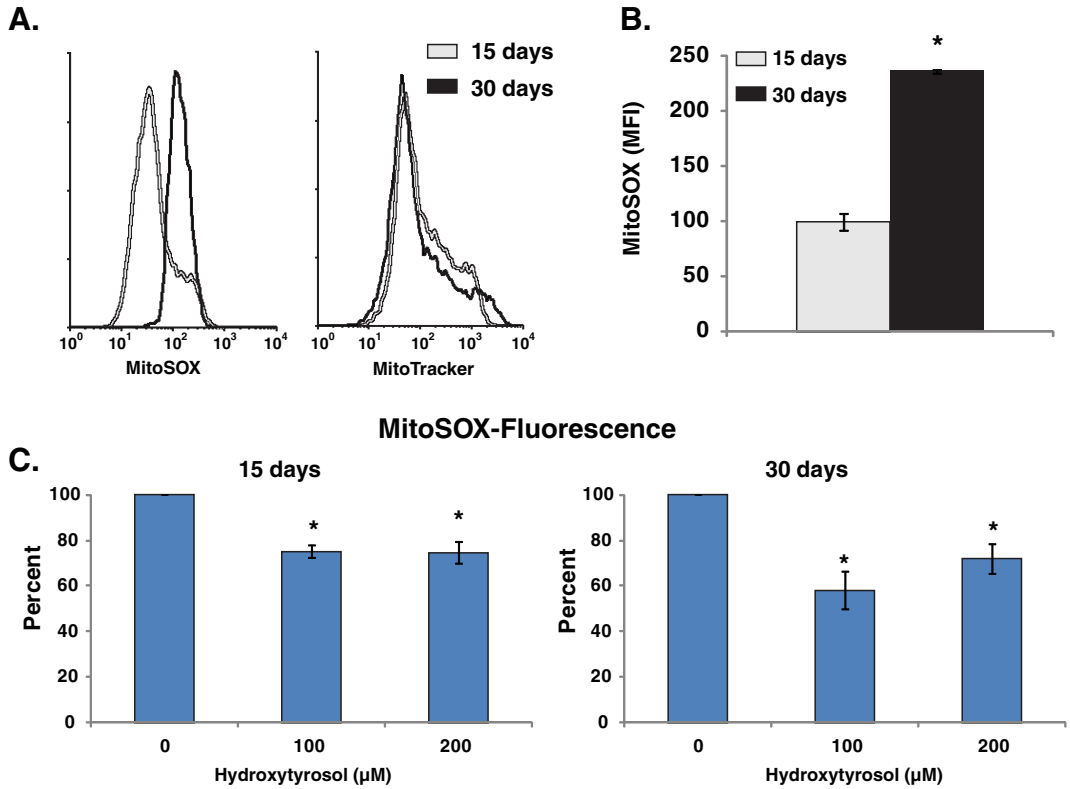

Fig. 5 Hydroxytyrosol suppresses age-associated accumulation of mitochondrial ROS during quiescence. Control and HT-treated 15- and 30-day quiescent NHFs were incubated with 10 μM MitoSOX and 0.5 μM MitoTracker green and fluorescence measured by flow cytometry following our previously published method (Sarsour et al. 2008). MitoSOX fluorescence was normalized to MitoTracker green fluorescence in each sample and percent change calculated relative to untreated control. **a** Representative histograms of MitoSox and MitoTracker in 15- and 30-day quiescent NHFs; **b** percent change in MitoSox fluorescence in 30- compared with 15-day untreated quiescent NHFs; **c** percent change in MitoSox fluorescence in HT-treated 15- and 30-day quiescent NHFs relative to untreated control. Asterisks indicate significant difference between HT-treated and untreated NHFs; $n=3$, $p<0.05$

myoglobin or hemoglobin, heme proteins that are well-known to have peroxidase activity (Fig. 6a).

Semiquinone radicals are the primary source for formation of superoxide from the hydroquinone–semiquinone–quinone triad (Eyer 1991; Song and Buettner 2010; Song et al. 2008; Venkatesha et al. 2008). If superoxide is formed in the oxidation of hydroquinones that have relatively high redox potentials, then superoxide dismutase will accelerate the oxidation of hydroquinone, forming quinone. HT was incubated in near-neutral buffer in presence or absence of superoxide dismutase and the change in absorbance was measured at 300 nm (the spectral region for the quinone form of HT). We observed that superoxide dismutase dramatically accelerated the oxidation of HT as seen by the rate of formation of HT–quinone (Fig. 6b); this unique experimental approach clearly demonstrates the formation of superoxide during the oxidation of HT. These results suggest that HT undergoes catechol–semiquinone–quinone redox cycling to generate superoxide, which in a biological system can activate the cellular antioxidant system.

Discussion

Our results show that continuous treatment with HT extends chronological lifespan in normal human skin fibroblasts. HT specifically induces MnSOD activity and suppresses age-associated increase in mitochondrial ROS levels. Although HT is an antioxidant, it can initially act as a prooxidant leading to the generation of superoxide and activation of MnSOD expression.

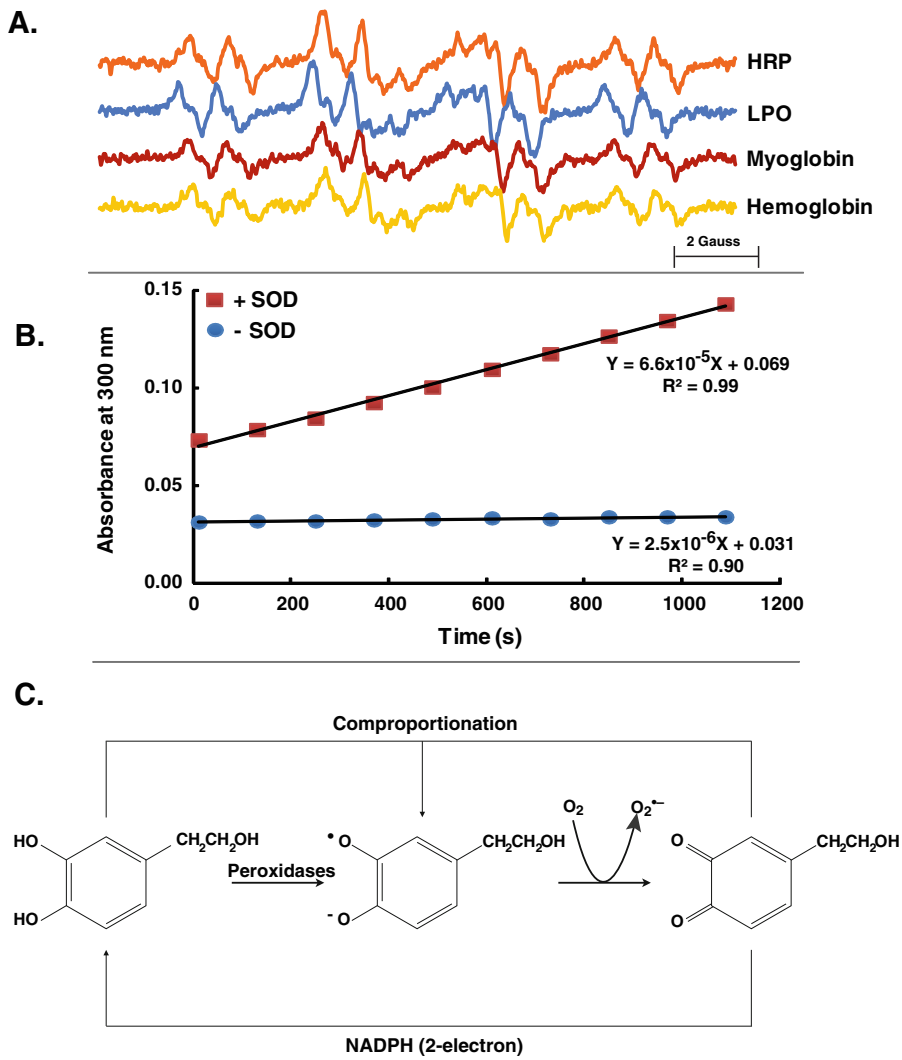

Fig. 6 Catechol–semiquinone–quinone redox cycling of hydroxytyrosol. **a** EPR spectra of the semiquinone radical of HT generated by 1 mM HT in PBS (pH 7.4) incubated with hydrogen peroxide and horseradish peroxidase (HRP), lactoperoxidase (LPO), myoglobin, or hemoglobin, and EPR spectra recorded. The EPR spectra are characterized by hyperfine splitting from three hydrogens on the aromatic ring with splitting constants of 3.7, 3.2, and 3.1 G, and two splittings from hydrogens not on the aromatic ring, 0.9 and 0.3 G. These hyperfine splittings are consistent with the structure of the semiquinone radical of HT. **b** UV spectroscopy measurement of HT–quinone formation during the autoxidation of HT was followed at 300 nm. **c** HT generates free radicals: in the presence of hydrogen peroxide, peroxidases oxidize HT to its semiquinone radical, which in turn leads to the formation of superoxide and quinone. The catechol–semiquinone–quinone triad can undergo redox cycling to generate a flux of superoxide

Previous literature showed that long duration of quiescence resulted in a significant loss in the proliferative capacity of NHFs (Munro et al. 2001; Sarsour et al. 2005; Sitte et al. 1998). We used contact-inhibited quiescent, but metabolically active cultures to study the effects of HT on CLS of NHFs. The metabolic activity was maintained by changing the media every 3 days with fresh media. Quiescent NHFs cultured in presence of HT were able to reenter the proliferative cycle even after 30- to 60-day of quiescence compared with the control cells that showed a significant decrease in their capacity to reenter the proliferative cycle (Figs. 1 and 2). There was no difference in the percentage of S and G_2 cells replated from control and 15-day HT-treated quiescent NHFs (Fig. 1), suggesting that the protective effects

of HT may not manifest early in quiescence. Alternatively, the molecular and cellular events initiating CLS may develop at a later stage of quiescence. NHFs replated from HT-treated 30- and 60-day quiescent cultures showed approximately 3-fold increase in the percentage of S and G_2 cells at 24–48-h post-plating compared with their respective time-matched controls (Figs. 1 and 2). Consistent with these results, cell population-doubling time was shorter in HT-treated cells compared with controls (32–38 vs. 51–57 h). The percentage of cells in S and G_2 phases of the cell cycle decreased to 10–20% in untreated control cells replated from 30- and 60-day quiescent cultures (Figs. 1 and 2), while cells replated from 3-day quiescent cultures exhibited 70% S and G_2 cells. These results suggest that approximately 50–60% of the quiescent population exit the cell cycle permanently during 30 to −60 days of quiescence.

Our results are comparable to that of Munro et al. (Munro et al. 2001) where the authors report loss of 15–25 population doublings in long-term quiescent cultures of normal human fibroblasts. This loss in population doublings was associated with approximately 94% of the cells exiting the cell cycle permanently. They showed that the loss in population-doubling in long-term quiescent cultures were not due to cell division and telomeric attrition. These results are consistent with earlier reports demonstrating an absence of telomere attrition in mid-lifespan fibroblasts that were kept in quiescent cultures for 7–10 weeks (Allsopp et al. 1995; Sitte et al. 1998). These results are also consistent with our earlier report where we demonstrated that MnSOD-induced extension of CLS was independent of telomerase activity (Sarsour et al. 2005). Interestingly, this irreversible exit from the cell cycle does not appear to be due to nutrient limitations because media was changed every 3 days in the quiescent cultures. However, it is possible that the permanent exit from the cell cycle in long-term quiescent cultures could be due to an age-associated decrease in cellular metabolism.

Several recent studies show a link between cellular metabolism and cell cycle progression (Mitra et al. 2009; Sarsour et al. 2010; Sarsour et al. 2008; Venkatesha et al. 2010; Wang et al. 2006). Cyclin D1 and E coordinate cell cycle progression with mitochondrial metabolism and functions (Mitra et al. 2009; Wang et al. 2006). Likewise, MnSOD dependent regulation of transition between quiescence and the proliferative cycle was associated with cyclin D1 and cyclin B1 protein levels (Sarsour et al. 2008); absence of MnSOD activity negatively impacts mitochondrial morphology and functions, which inhibits quiescent NHFs entry into the proliferative cycle (Sarsour et al. 2010). An inverse correlation was observed between cyclin D1 protein levels and glucose consumption in oxidatively stressed cells (Venkatesha et al. 2010). These results support the hypothesis that cellular metabolism regulates cell proliferation. Although additional research is needed to determine if age-associated changes in cellular metabolism could influence CLS, our results support the hypothesis of a "metabolic time" (Goldstein and Singal 1974) regulating the CLS-dependent ageing.

Results presented in Figs. 3 and 4 show that MnSOD activity regulates HT-induced extension of CLS. HT has been shown recently to increase superoxide dismutase, catalase, and glutathione peroxidase activity in the liver and kidney of diabetic rats (Hamden et al. 2009). Indeed, a significant increase in MnSOD activity, protein, and mRNA levels was observed in HT-treated quiescent cultures of NHFs (Fig. 3). HT treatments did not show any change in CuZnSOD activity or protein levels of CuZnSOD, GPx, and catalase. These results suggest the protective role of HT could be due to its ability to activate the expression of MnSOD (Fig. 3). The percentage of S and G_2 in cell-populations replated from 3-day quiescent NHFs overexpressing a dominant-negative mutant form of MnSOD was approximately 10% compared with 70% in uninfected and AdBgl II infected controls (Fig. 4). HT treatments partially recovered the percentage of S and G_2 cells in AdmMnSOD-infected NHFs. These results are comparable to our previously published results of MnSOD overexpression extending CLS in fibroblasts (Sarsour et al. 2005) and that of Harris et al. (Harris et al. 2003) demonstrating MnSOD overexpression extending CLS in *S. cerevisiae*.

MnSOD is localized in the mitochondrial matrix and removes mitochondrial generated superoxide. Therefore, mitochondrial functions could regulate HT-induced extension of CLS. Mitochondrial ROS levels increased approximately 2-fold in 30- vs. 15-day quiescent NHFs (Fig. 5b). HT treatments suppressed an age-associated increase in mitochondrial ROS levels by approximately 25–50% (Fig. 5c). We have shown previously that age-associated increase in

mitochondrial ROS of quiescent NHFs was associated with significant abnormalities in mitochondrial morphology including loss of cristae formation (Sarsour et al. 2010). Interestingly, overexpression of MnSOD suppressed ROS accumulation, protected mitochondrial morphology from age-associated abnormalities, and extended CLS. We hypothesize that HT-induced activation of MnSOD expression protects mitochondrial morphology from age-associated abnormalities, which then leads to the extension of CLS. Furthermore, these results also provide additional evidence in support of the "metabolic time" concept of cellular ageing. While replicative senescence is dependent on "mitotic counting" and "telomere attrition" mechanisms, our results suggest CLS is governed by "metabolic time" which could be responsive to age-associated changes in cellular metabolism.

Several studies report the antioxidant properties of HT in biological systems (Cornwell and Ma 2008; D'Angelo et al. 2005; Hamden et al. 2009; Jemai et al. 2009; Manna et al. 1999; O'Dowd et al. 2004; Visioli et al. 1998). However, the mechanisms leading to the antioxidant properties of HT are not completely understood. Results from the present study suggest that the antioxidant properties of HT could be due to its ability to act initially as a prooxidant leading to the generation of free radicals; cells respond to this flux in free radicals by activating the expression of antioxidant enzymes. HT may promote reduction of hydrogen peroxide to water by acting as a substrate for cellular peroxidases, generating the HT–semiquinone radical (Fig. 6a, c). Oxidation of the HT–semiquinone radical to HT–quinone generates superoxide. Results presented in Fig. 6 support this hypothesis. The formation of HT–quinone was observed using UV spectrometry in presence and absence of SOD. In the absence of SOD, the autoxidation of HT to quinone was relatively slow (Fig. 6b). However, SOD dramatically accelerated the oxidation of HT as seen by the rate of formation of HT–quinone (Fig. 6b). HT–quinone may interact with HT in a comproportionation reaction to generate more semiquinone radicals (Song and Buettner 2010; Song et al. 2008; Song et al. 2009). This redox cycle of HT could elicit an oxidative stress response and cells may adapt to this oxidative insult by promoting their antioxidant defense system.

In summary, our results show HT, a major polyphenol in olive oil, extends CLS in fibroblasts by enhancing MnSOD activity thereby suppressing an age-associated accumulation of mitochondrial ROS. The antioxidant properties of HT could be due to its catechol–semiquinone–quinone redox cycling properties leading to a prooxidant environment, which then activates the cellular antioxidant defense system (Fig. 7). These results are also of significance in vivo

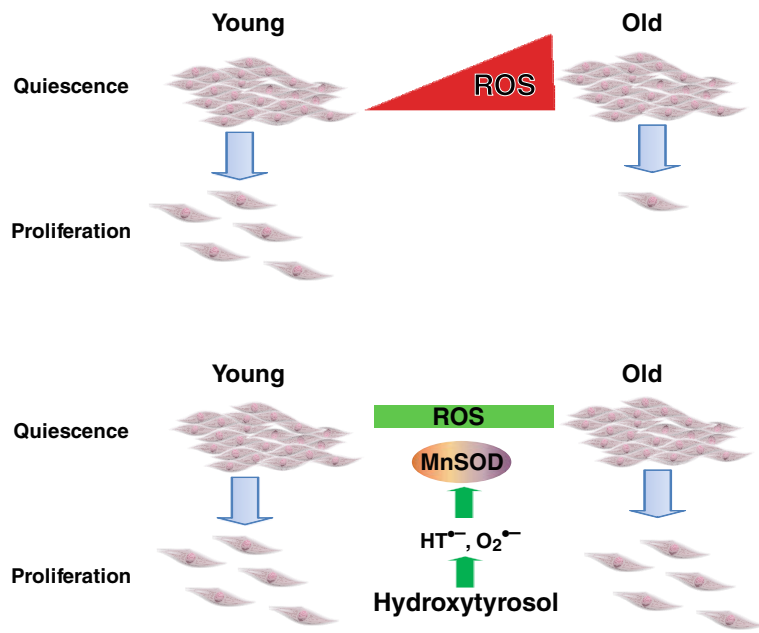

Fig. 7 MnSOD activity regulates hydroxytyrosol-induced extension of chronological lifespan. Hydroxytyrosol undergoes catechol–semiquinone–quinone redox cycling that results in the generation of superoxide, which then activates the cellular antioxidant defense system. HT-induced activation of MnSOD activity suppresses age-associated accumulation of mitochondrial ROS leading to an extension of CLS in normal human fibroblasts

in understanding the molecular and cellular biology of quiescence. Adult stem cells, progenitor cells of the bone marrow, and cells in the liver and intestines are a few examples of cellular quiescence in vivo. The extended CLS and ability to remain in quiescence may be responsible for their longevity. It would be of interest to know if CLS is present in stem cells and whether antioxidants extend CLS thereby facilitating cell and tissue renewal. Finally, the quiescent cell culture system used in our study can be adapted to investigate the cellular and molecular biology of CLS, which is distinct from the "mitotic counting" and "telomere attrition" pathways of replicative senescence.

Acknowledgments We thank The University of Iowa EPR and Flow Cytometry Cores for assisting with EPR spectroscopy and flow cytometry assays. Funding from NIH CA 111365 and McCord Research foundation supported this work.

References

Allsopp RC, Chang E et al (1995) Telomere shortening is associated with cell division in vitro and in vivo. Exp Cell Res 220:194–200. doi:10.1006/excr.1995.1306

Bachur NR, Gordon SL, Gee MV (1978) A general mechanism for microsomal activation of quinone anticancer agents to free radicals. Cancer Res 38:1745–1750

Beauchamp C, Fridovich I (1971) Superoxide dismutase: improved assays and an assay applicable to acrylamide gels. Anal Biochem 44:276–287

Bodnar AG, Ouellette M et al (1998) Extension of life-span by introduction of telomerase into normal human cells. Science 279:349–352

Buettner GR, Ng CF et al (2006) A new paradigm: manganese superoxide dismutase influences the production of H_2O_2 in cells and thereby their biological state. Free Radic Biol Med 41:1338–1350. doi:10.1016/j.freeradbiomed.2006.07.015

Cornwell DG, Ma J (2008) Nutritional benefit of olive oil: the biological effects of hydroxytyrosol and its arylating quinone adducts. J Agric Food Chem 56:8774–8786. doi:10.1021/jf8015877

D'Angelo S, Ingrosso D et al (2005) Hydroxytyrosol, a natural antioxidant from olive oil, prevents protein damage induced by long-wave ultraviolet radiation in melanoma cells. Free Radic Biol Med 38:908–919. doi:10.1016/j.freeradbiomed.2004.12.015

De Lucia M, Panzella L et al (2006) Oxidative chemistry of the natural antioxidant hydroxytyrosol: hydrogen peroxide-dependent hydroxylation and hydroxyquinone/o-quinone coupling pathways. Tetrahedron 62:1273–1278. doi:10.1016/j.tet.2005.10.055

Eyer P (1991) Effects of superoxide dismutase on the autoxidation of 1,4-hydroquinone. Chem Biol Interact 80:159–176

Fabiani R, Rosignoli P et al (2008) Oxidative DNA damage is prevented by extracts of olive oil, hydroxytyrosol, and other olive phenolic compounds in human blood mononuclear cells and HL60 cells. J Nutr 138:1411–1416

Fabrizio P, Pletcher SD et al (2004) Chronological aging-independent replicative life span regulation by Msn2/Msn4 and Sod2 in *Saccharomyces cerevisiae*. FEBS Lett 557:136–142

Goldstein S, Singal DP (1974) Senescence of cultured human fibroblasts: mitotic versus metabolic time. Exp Cell Res 88:359–364

Hamden K, Allouche N, Damak M, Elfeki A (2009) Hypoglycemic and antioxidant effects of phenolic extracts and purified hydroxytyrosol from olive mill waste in vitro and in rats. Chem Biol Interact 180:421–432. doi:10.1016/j.cbi.2009.04.002

Harris N, Costa V et al (2003) Mnsod overexpression extends the yeast chronological (G(0)) life span but acts independently of Sir2p histone deacetylase to shorten the replicative life span of dividing cells. Free Radic Biol Med 34:1599–1606.

Hayflick L, Moorhead PS (1961) The serial cultivation of human diploid cell strains. Exp Cell Res 25:585–621

Henderson ER, Larson DD (1991) Telomeres—what's new at the end? Curr Opin Genet Dev 1:538–543

Jemai H, Fki I et al (2008) Lipid-lowering and antioxidant effects of hydroxytyrosol and its triacetylated derivative recovered from olive tree leaves in cholesterol-fed rats. J Agric Food Chem 56:2630–2636. doi:10.1021/jf072589s

Jemai H, El Feki A, Sayadi S (2009) Antidiabetic and antioxidant effects of hydroxytyrosol and oleuropein from olive leaves in alloxan-diabetic rats. J Agric Food Chem 57:8798–8804. doi:10.1021/jf901280r

Manna C, Della Ragione F et al (1999) Biological effects of hydroxytyrosol, a polyphenol from olive oil endowed with antioxidant activity. Adv Exp Med Biol 472:115–130

Menon SG, Sarsour EH et al (2003) Redox regulation of the G1 to S phase transition in the mouse embryo fibroblast cell cycle. Cancer Res 63:2109–2117

Mitra K, Wunder C et al (2009) A hyperfused mitochondrial state achieved at G1-S regulates cyclin E buildup and entry into S phase. Proc Natl Acad Sci USA 106:11960–11965. doi:10.1073/pnas.0904875106

Mukherjee S, Lekli I et al (2009) Expression of the longevity proteins by both red and white wines and their cardioprotective components, resveratrol, tyrosol, and hydroxytyrosol. Free Radic Biol Med 46:573–578. doi:10.1016/j.freeradbiomed.2008.11.005

Munro J, Steeghs K et al (2001) Human fibroblast replicative senescence can occur in the absence of extensive cell division and short telomeres. Oncogene 20:3541–3552. doi:10.1038/sj.onc.1204460

O'Dowd Y, Driss F et al (2004) Antioxidant effect of hydroxytyrosol, a polyphenol from olive oil: scavenging of hydrogen peroxide but not superoxide anion produced by human neutrophils. Biochem Pharmacol 68:2003–2008. doi:10.1016/j.bcp.2004.06.023

Orr WC, Mockett RJ, Benes JJ, Sohal RS (2003) Effects of overexpression of copper-zinc and manganese superoxide dismutases, catalase, and thioredoxin reductase genes on

longevity in *Drosophila melanogaster*. J Biol Chem 278:26418–26422. doi:10.1074/jbc.M303095200

Rodriguez G, Lama A et al (2009) 3,4-Dihydroxyphenylglycol (DHPG): an important phenolic compound present in natural table olives. J Agric Food Chem 57:6298–6304. doi:10.1021/jf803512r

Sarsour EH, Agarwal M et al (2005) Manganese superoxide dismutase protects the proliferative capacity of confluent normal human fibroblasts. J Biol Chem 280:18033–18041. doi:10.1074/jbc.M501939200

Sarsour EH, Venkataraman S et al (2008) Manganese superoxide dismutase activity regulates transitions between quiescent and proliferative growth. Aging Cell 7:405–417. doi:10.1111/j.1474-9726.2008.00384.x

Sarsour EH, Goswami M, Kalen AL, Goswami PC (2010) MnSOD activity protects mitochondrial morphology of quiescent fibroblasts from age associated abnormalities. Mitochondrion 10:342–349. doi:10.1016/j.mito.2010.02.004

Schriner SE, Linford NJ et al (2005) Extension of murine life span by overexpression of catalase targeted to mitochondria. Science 308:1909–1911. doi:10.1126/science.1106653

Sitte N, Saretzki G, von Zglinicki T (1998) Accelerated telomere shortening in fibroblasts after extended periods of confluency. Free Radic Biol Med 24:885–893

Sohal RS, Sohal BH, Orr WC (1995) Mitochondrial superoxide and hydrogen peroxide generation, protein oxidative damage, and longevity in different species of flies. Free Radic Biol Med 19:499–504

Song Y, Buettner GR (2010) Thermodynamic and kinetic considerations for the reaction of semiquinone radicals to form superoxide and hydrogen peroxide. Free Radic Biol Med. doi:10.1016/j.freeradbiomed.2010.05.009

Song Y, Wagner BA, Lehmler HJ, Buettner GR (2008) Semiquinone radicals from oxygenated polychlorinated biphenyls: electron paramagnetic resonance studies. Chem Res Toxicol 21:1359–1367. doi:10.1021/tx8000175

Song Y, Wagner BA et al (2009) Nonenzymatic displacement of chlorine and formation of free radicals upon the reaction of glutathione with PCB quinones. Proc Natl Acad Sci USA 106:9725–9730. doi:10.1073/pnas.0810352106

Sun J, Folk D, Bradley TJ, Tower J (2002) Induced overexpression of mitochondrial Mn-superoxide dismutase extends the life span of adult *Drosophila melanogaster*. Genetics 161:661–672

Taub J, Lau JF et al (1999) A cytosolic catalase is needed to extend adult lifespan in *C. elegans* daf-C and clk-1 mutants. Nature 399:162–166. doi:10.1038/20208

Vaziri H, Benchimol S (1998) Reconstitution of telomerase activity in normal human cells leads to elongation of telomeres and extended replicative life span. Curr Biol 8:279–282

Venkatesha VA, Venkataraman S et al (2008) Catalase ameliorates polychlorinated biphenyl-induced cytotoxicity in nonmalignant human breast epithelial cells. Free Radic Biol Med 45:1094–1102. doi:10.1016/j.freeradbiomed.2008.07.007

Venkatesha VA, Kalen AL, Sarsour EH, Goswami PC (2010) PCB-153 exposure coordinates cell cycle progression and cellular metabolism in human mammary epithelial cells. Toxicol Lett 196:110–116. doi:10.1016/j.toxlet.2010.04.005

Visioli F, Bellomo G, Galli C (1998) Free radical-scavenging properties of olive oil polyphenols. Biochem Biophys Res Commun 247:60–64. doi:10.1006/bbrc.1998.8735

Vogna D, Pezzella A et al (2003) Oxidative chemistry of hydroxytyrosol: isolation and characterisation of novel methanooxocinobenzodioxinone derivatives. Tetrahedron Lett 44:8289–8292. doi:10.1016/j.tetlet.2003.09.066

Wang C, Li Z et al (2006) Cyclin D1 repression of nuclear respiratory factor 1 integrates nuclear DNA synthesis and mitochondrial function. Proc Natl Acad Sci USA 103:11567–11572. doi:10.1073/pnas.0603363103

Wright WE, Brasiskyte D, Piatyszek MA, Shay JW (1996) Experimental elongation of telomeres extends the lifespan of immortal×normal cell hybrids. EMBO J 15:1734–1741

Yamada K, Ogawa H et al (2009) Mechanism of the antiviral effect of hydroxytyrosol on influenza virus appears to involve morphological change of the virus. Antivir Res 83:35–44. doi:10.1016/j.antiviral.2009.03.002

Zhang YP, Smith BJ, Oberley LW (2006) Enzymatic activity is necessary for the tumor-suppressive effects of MnSOD. Antioxid Redox Signal 8:1283–1293